Pulsed-field ionization spectroscopy of high Rydberg states (n=50–200) of bis(η^6-benzene)chromium

Kyo-Won Choi, Sunyoung Choi, Sun Jong Baek, and Sang Kyu Kim[a)]
Department of Chemistry and School of Molecular Sciences (BK21), Korea Advanced Institute of Science and Technology (KAIST), Daejeon 301-750, Korea

(Received 12 October 2006; accepted 22 November 2006; published online 17 January 2007)

The ionization behavior of the high Rydberg states of bis(η^6-benzene)chromium in the presence of ac and/or dc fields has been explored. The application of an ac scrambling field at the time of laser excitation lengthens the lifetime of the Rydberg state by almost two orders of magnitude. The lifetime enhancement by the scrambling field is much more effective for $n<100$ than it is for $n>100$ Rydberg states. The pulsed-field ionization of Rydberg states of $n<100$ shows the typical diabatic ionization behavior for low n. The two distinct ionization behaviors observed for the relatively low (n=50–100) and high (n=100–200) Rydberg states suggest that the former originate from the optically accessed nf Rydberg series, whereas the latter are due to np Rydberg series. Based on the understanding of the ionization behavior of bis(η^6-benzene)chromium, the accurate ionization potential is deduced to give IP=5.4665±0.0003 eV. Optimization of the various electric field conditions greatly enhances the spectral sensitivity of the mass-analyzed threshold ionization (MATI) spectroscopy. The high-resolution MATI spectrum of the title molecule obtained here provides precise cationic vibrational frequencies for many skeletal and benzene ring modes. A number of vibrational modes are newly identified, and the ambiguity regarding to some mode assignments is now clearly resolved through the Frank-Condon analysis based on *ab initio* calculations. © *2007 American Institute of Physics*. [DOI: 10.1063/1.2423022]

I. INTRODUCTION

Pulsed-field ionization (PFI) of high Rydberg states of atoms and molecules has been a hot topic especially in the late 1990s,[1–18] since excellent spectroscopic tools such as zero-electron kinetic energy (ZEKE) or mass-analyzed threshold ionization (MATI) spectroscopy rely on the PFI of long-lived high n Rydberg states.[18–28] The mechanism of the enormous lifetime lengthening of high Rydberg states has been subjected to intensive investigation for many chemical systems.[1,2,29] Through a number of excellent experimental and theoretical studies, it is now well accepted that the lifetime lengthening is mainly due to the l mixing induced by a stray field which cannot be easily avoided in most laboratories.

The l mixing from the optically prepared low-l state gives rise to the population in the nonpenetrating high-l states in which the electron orbits like that of hydrogen. The binding energy of an electron is expressed by the following relation:

$$E_{n\ell} = -\frac{R_M}{(n-\delta_\ell)^2}.$$

Here, R_M is the Rydberg constant, n the principal quantum number, and δ_l the l-dependent quantum defect. The higher l gives the smaller δ_l, implying that the corresponding electronic wave function is less overlapped with the ionic core to significantly slow down the dephasing processes of Rydberg states via predissociation, internal conversion, or autoionization.[1,2,4,5]

Experimentally, an n^4 dependence of the high n Rydberg state lifetime has been regarded as the evidence for the field-induced l mixing, while the collisional m_l mixing is considered to be responsible for an n^5 dependence.[1,5] Even though many experimental observations have been successfully explained by theoretical models developed by Levine and co-workers,[6,7] the PFI behavior of high n Rydberg states of molecules is quite complex and it is not well understood yet. For example, in many cases, the application of a small dc field at the time of laser excitation is known to diminish the Rydberg state lifetime of molecules,[12–16] while the opposite cases have also been reported.[17] The l mixing induced by a small dc field has been thoroughly studied for NO by Vrakking and Lee.[5] They reported the minimum electric field required to induce the l mixing for nf or np Rydberg series of NO which are prepared by the $(1+1')$ two-photon excitation. The np series of NO has the δ value of 0.7286, whereas the quantum defect of nf series was found to be much smaller to give δ_l=0.0101. The more hydrogeniclike feature of the nf series has been manifested in the lower n and electric field values required for the l mixing to effectively occur compared with those for np series.[5]

Compared to the case of NO, the ionization behavior of high Rydberg states of polyatomic molecules is much less understood. One of the reasons would be the increase of the number of degrees of freedom which results in the lifetime shortening of high n Rydberg states. Even though ZEKE spectroscopy has been widely used for accurate ionization

[a)]Author to whom correspondence should be addressed. Electronic mail: sangkyukim@kaist.ac.kr

potential (IP) measurements in the sense that it probes the Rydberg states of $n>250$ using the small extraction field, the mechanism of l mixing of high n states prior to PFI has little been studied for polyatomic molecules. Nonetheless, it should be noted that the long-lived Rydberg manifolds for Ar, HCl, N_2, C_6H_6, and O_2 were investigated by Hofstein *et al.*[18] using the MATI spectroscopy. They pointed out the importance of the initially prepared Rydberg orbital for the understanding of the varying widths of Rydberg manifolds of different molecules. Additionally, it is also noteworthy that high Rydberg states ($n>50$) of 1,4-diazabicyclo [2,2,2] octane (DABCO) and DABCO-N_2 have been identified and their ionization behavior was studied using ZEKE and/or MATI spectroscopic techniques.[9–11]

Here, we have studied the ionization behavior of high Rydberg states of bis(η^6-benzene)chromium, $Cr(Bz)_2$. In spite of the large size of this molecule, the Rydberg transitions up to $n=35$ had been clearly observed to give the quantum defect and extrapolated IP values.[9] For Rydberg states of $n>35$, presumably due to the overlap with intervalence transitions, no spectroscopic information is available to date. In this work, using the delayed pulsed-field ionization technique, Rydberg states of $n=50-200$ are identified for the first time. The stray or ac scrambling field greatly enhances the Rydberg state lifetime, enabling one to observe high n Rydberg states and their ionization behavior. The high-resolution MATI spectrum is taken to give the detailed vibrational structure of the $Cr(Bz)_2$ cation. In this work, we greatly improved the spectral resolution of the MATI spectrum of $Cr(Bz)_2$ compared with other previous works,[23,26–28] resolving the earlier ambiguity in the vibrational mode assignment. Furthermore, our MATI spectrum provides many newly found vibrational frequencies which are essential for the understanding of the nature of the metal-benzene η bonding.

II. EXPERIMENT

Bis(η^6-benzene)chromium was purchased from Aldrich (97%) and used without further purification. The experimental setup has been described earlier[19,24,25] and is only briefly given here. The sample was heated to 120 °C, mixed with Ar carrier gas, and expanded into vacuum through a 0.8 mm diameter nozzle orifice (General Valve 9 Series). The supersonic jet was then skimmed though a 1 mm diameter skimmer (Precision Instrument) before it was collinearly overlapped with the UV laser pulse. The backing pressure was ~1.5 atm and the background pressure of $\sim 10^{-7}$ Torr was maintained when the nozzle was on. A tunable laser pulse (1–2 mJ/pulse, $\Delta t=\sim 6$ ns) in the 220–228 nm range was generated by the frequency doubling of the laser output from a dye laser (Lambda Physik, Scanmate 2) pumped by the third harmonic output of a Nd:YAG laser (Continuum, Precision II) through a BBO crystal placed on a homemade autotracker.

Molecules were excited to high n Rydberg states and allowed to stay for 10–200 μs before they were ionized by the pulsed field of 10–100 V/cm to give MATI ions. Because of the long delay time between the laser irradiation and pulsed-field ionization, the direct ions were spread out to be completely separated from the MATI ions. Resultant MATI ions were accelerated, drifted along the field-free region, and detected by dual microchannel plates. Ion signals were digitized by a digital oscilloscope (LeCroy, LT584M) and stored in a personal computer using a data-taking program which controls the dye laser frequency tuning and homemade autotracker as well. Various electric field conditions were applied to explore the ionization behavior of high Rydberg states. For the ac scrambling field, the ac noise accompanied with the high-voltage pulser (DEI, PVM-4140) was used. The spoil field of 0.01–4 V/cm was applied when its effect on the MATI signal was investigated. For the high-resolution MATI spectrum, the electric field scheme in Fig. 1 was used. No spoil field was used, whereas the ac scrambling field was applied at the time of laser irradiation. The pulsed field of 10 V/cm was used to ionize and repel MATI ions into the accelerating field. Further acceleration was carried out in the upper electrodes for recording the frequency-dependent MATI signal.

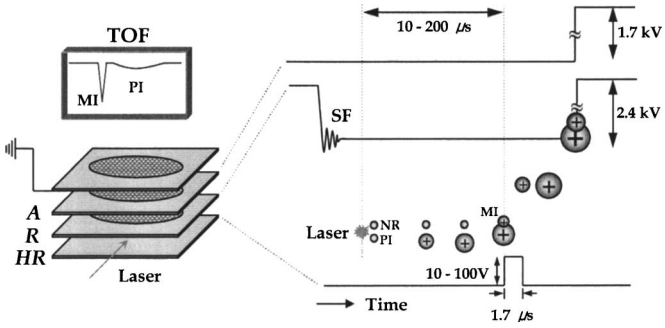

FIG. 1. Experimental scheme for taking the high-resolution MATI spectrum. PI: prompt ion, MI: MATI ion, NR: neutral Rydberg, SF: scrambling field, HR: plate for the high resolution, R: repeller plate, and A: accelerator plate.

Ab initio calculations were carried out by using the GAUSSIAN 03W program package.[30] The geometry and vibrational frequency of neutral and cationic states of bis(η^6-benzene)chromium were calculated using the Möller-Plesset second-order perturbation theory and density functional theory (B3LYP) with the pseudo-core-potential LANL2DZ basis set. All harmonic frequencies reported here are not scaled. Frank-Condon overlap integrals using the Duschinsky transformation[31] are calculated with a code developed by Peluso *et al.*[32] and Borrelli and Peluso.[33] Optimized structures and normal mode frequencies are used as inputs for both neutral and cationic states.

III. RESULTS AND DISCUSSION

One-photon MATI spectrum of $Cr(Bz)_2$ obtained in this work is compared with that previously reported by our group,[23] Fig. 2. The MATI spectrum in Fig. 2(a), which was taken with the pulsed field (F) of ~400 V/cm, shows broad spectral features, whereas the high-resolution MATI spectrum taken with $F=10$ V/cm consists of sharp peaks with the narrow full width at half maximum bandwidth of ~ 5 cm^{-1}. The spectral narrowing by the smaller pulse-field strength is natural as the energy range of Stark states subjected to ionization becomes narrower with decreasing the pulse-field strength. However, the distinct structure observed

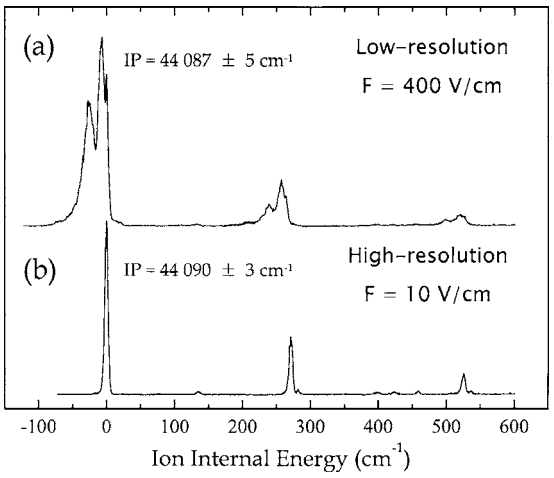

FIG. 2. (a) The low-resolution (from Ref. 23) and (b) the high-resolution MATI spectrum of the bis(η^6-benzene)chromium.

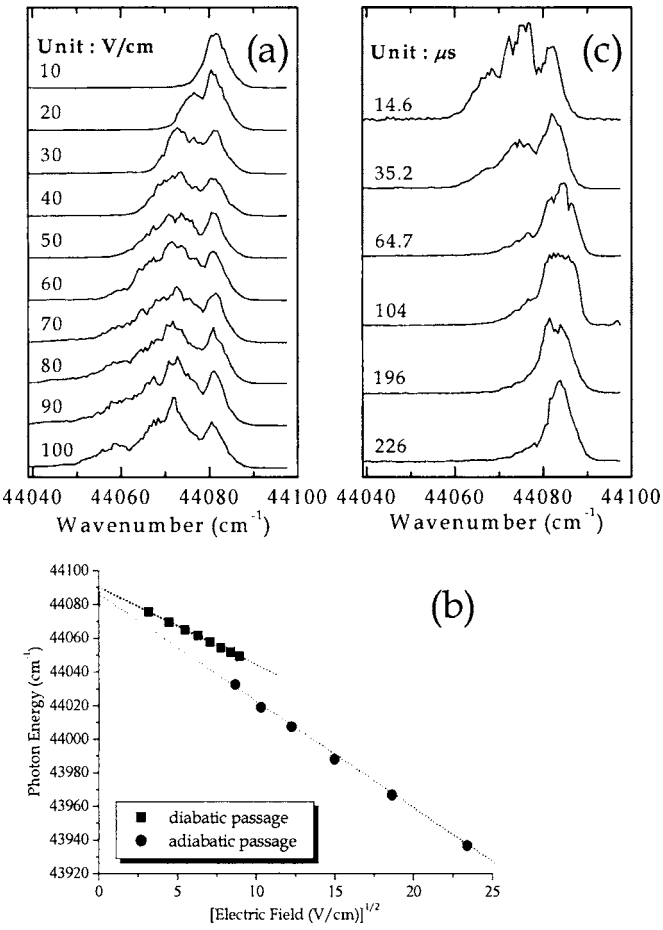

FIG. 3. (a) MATI origin bands recorded at various pulsed-field strengths. The delay time between the laser irradiation and PFI is fixed at 14 μs. (b) The plot of the ionization onset energy vs the square root of the pulsed field, showing the diabatic ($\Delta IP \sim 4.54\sqrt{F}$) or adiabatic ($\Delta IP \sim 6.41\sqrt{F}$) ionization pathway. For the latter, the ionization threshold energy for the formation of direct ions is monitored. (c) MATI origin bands taken as a function of the delay time between the laser irradiation and PFI. The pulsed field is fixed at 50 V/cm.

in the vibronic band in Fig. 2(a) is unusual and the origin of the structure needs to be investigated. The spectral structure observed in the red wing of the band in Fig. 2(a) had also been observed in the ZEKE spectrum reported in Ref. 9, in which it was ascribed to the autoionizing rotational states. Sohnlein and Yang, in their recent ZEKE spectroscopic work,[26] reported a similar-shaped band in which the structure was attributed to a low-frequency vibrational mode. Since they used laser ablation to produce the internally hot $Cr(Bz)_2$, however, the direct comparison with the MATI spectrum in Fig. 2(a) is not adequate.

Here, we examine spectral changes for various combinations of applied electric fields. The origin of the MATI spectral structure is associated with two distinct ionization behaviors of two different *nl* series. The high-resolution MATI spectrum, after resolving the issue of the ionization behavior of high *n* Rydberg states of $Cr(Bz)_2$, provides not only the most precise vibrational frequencies for the modes already identified before but also accurate frequency values for many other vibrational modes.

A. Ionization behavior of high Rydberg states (n=50–200) of the bis(η^6-benzene)chromium

The application of an ac scrambling field at the laser irradiation time greatly enhances the lifetime of Rydberg states. As the PFI strength (F) increases, according to the diabatic ionization mechanism, the ionization window becomes widened to ionize the Stark states down to IP $\sim 4\sqrt{F}$ cm^{-1}.[1,2,29] The MATI origin band obtained as a function of the PFI strength is shown in Fig. 3(a). The delay time between the laser and PFI is fixed at 14 μs. Interestingly, as the PFI strength increases the shoulder at the red wing starts to appear and it becomes a distinct peak at $F > 30$ V/cm. Consequently, for example, at $F=100$ V/cm, two distinct peaks are observed over the energy range of $\sim$50 cm^{-1}. A broad band centered at $\sim$44 072 cm^{-1} shows a gradual decrease of its bandwidth, accompanied by the blueshift of its red edge as the pulsed-field strength decreases. The shift of the red edge of the band with F (V/cm) follows the relation $\Delta IP \sim 4.54\sqrt{F}$, giving an adiabatic IP value of 44 090±3 cm^{-1}, Fig. 3(b). The ionization behavior is consistent with a diabatic ionization model mechanism for low *n*. Meanwhile, the relatively sharp band located at 44 080 cm^{-1} shows little change with the change of pulsed-field strength. At $F=10$ V/cm, the broad band feature disappears while only a sharp band remains. Because of the long delay time between the laser excitation and pulsed-field ionization, no spoil field is used. It is clear that the band structure of the red shoulder in Fig. 2(a) is not due to the internal states of $Cr(Bz)_2$. Rather, it should be ascribed to the relatively low *n* Rydberg states of $Cr(Bz)_2$. Furthermore, it seems that the ionization behavior of Rydberg states is quite different for low and high *n* Rydberg states.

In order to investigate the origin for two distinct PFI behaviors, many different combinations of electric fields were explored. In Fig. 3(c), the pulsed field is fixed at 50 V/cm and the delay time between the laser and rising edge of the PFI voltage is changed to monitor the associated change of the MATI band shape. Although an accurate lifetime cannot be deduced from this measurement, it is obvious that the lifetime of the red shoulder is shorter than that of the peak at the blue edge. That is, the red-shoulder intensity

TABLE I. Experimental ionization potentials of bis(η^6-benzene)chromium.

IP (cm^{-1})	Method	Ref./year
44 090±3	High-resolution MATI spectroscopy	This work
44 081±7	ZEKE spectroscopy	26/2006
44 087±5	One-photon MATI spectroscopy	23/2004
44 087±3	Two-photon MATI spectroscopy	28/2004
44 020±30	Gas-phase photoabsorption	35/1997
44 090.3±0.5	Rydberg states fitting	9/1994

decreases sharply at around the delay time of 60 μs, whereas the peak at ~44 080 cm^{-1} remains almost the same even at the delay time of ~200 μs. It is quite amazing that the MATI signal survives even at ~226 μs after the laser excitation. Considering our experimental apparatus in which the laser excitation is collinearly overlapped with the molecular beam, the MATI signal obtained at $\Delta t \sim 226$ μs indicates that the long-lived Rydberg state is prepared at ~22.6 cm away from the center of the electrode if the velocity of 1 km/s is assumed for the supersonic jet. The length of the electrode is 5 cm, thus the MATI signal at $\Delta t \sim 226$ μs should come from molecules which were 18.6–22.6 cm away from the electrode assembly at the time of excitation. Therefore, the MATI band observed at $\Delta t > 186$ μs is not due to the effect of the ac scrambling field, which is applied at the laser irradiation time. The 3–4 cm^{-1} blueshift of the peak position at $\Delta t \sim 226$ μs, therefore, indicates that the dc field used in this work has caused the removal of the high n Rydberg states by the adiabatic ionization of Stark states. This experimental fact suggests that the dc field should be employed very carefully especially for the accurate IP measurement.

If the extrapolated IP value in the plot of the diabatic ionization threshold versus $\sqrt{F}$ is taken to be the adiabatic IP, approximate principal quantum numbers can be calculated for the signals at different energies. For low n (<35) Rydberg series, it was reported that the extrapolated IP value is 44 090 cm^{-1} and $\delta = 1.38$ for np series.[9] The IP value in Ref. 9 is in excellent agreement with our value. The IP values determined by various methods are compiled in Table I. The quantum defect is strongly l dependent, and it is nontrivial in our work to determine δ_l since Rydberg states are not well resolved. For high n, however, the δ_l value becomes less important in the Rydberg formula. Accordingly, when δ_l is assumed to be zero, the MATI signal observed at $F = 100$ V/cm represents the Rydberg states in the range of $n = 50–200$, as depicted in Fig. 4(a). It is then clear that the peak on the red side corresponds to the Rydberg states in the range of $n = 50–100$, while the peak on the blue side represents the $n = 100–200$ Rydberg states. It is quite obvious that the onset value of n for the lifetime lengthening is relatively low for the peak in the $n = 50–100$ range compared to that for the $n = 100–200$ Rydberg states. It should be noted that the MATI signal intensity decreases at around $n \sim 100$, suggesting that the lifetime gets shortened at corresponding states. Even though we could not resolve individual Rydberg lines, these experimental findings suggest that two distinct peaks at different n values in Fig. 4(a) have different initial l quantum numbers.

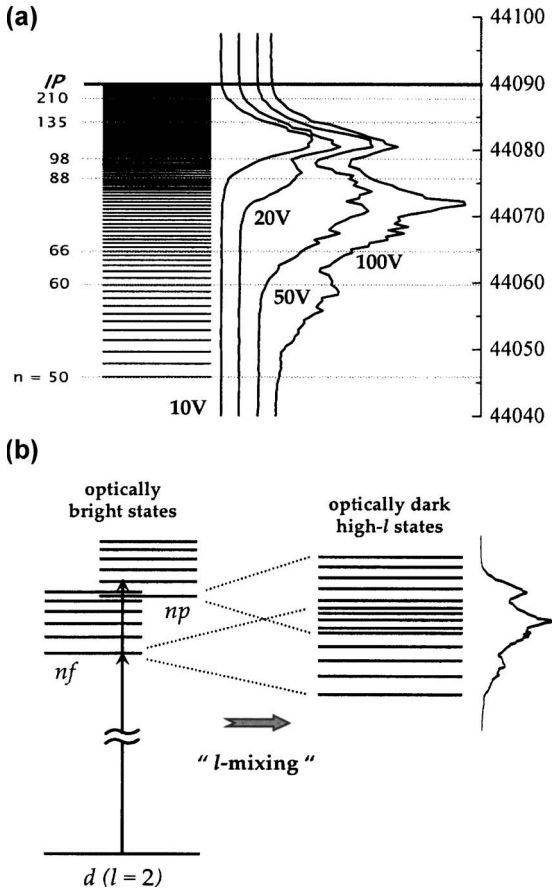

FIG. 4. (a) The approximate principal quantum numbers corresponding to the MATI peaks taken at various pulsed-field strengths. The adiabatic IP of 44 090 cm^{-1} is used while $R_\infty = 109\,737$ cm^{-1} and $\delta = 0$ are assumed in the Rydberg formula. (b) Initially prepared optically bright nf and np Rydberg series are strongly coupled to high-l long-lived states to give the resultant MATI bands (see the text).

In other words, the $n = 50–100$ Rydberg states may belong to the nf series in which the initial l quantum number is 3, whereas the $n = 100–200$ Rydberg states correspond to np series where the initial l is equal to 1. Similarly to the case of NO,[5] the nf series is more hydrogenic and the l mixing occurs at the lower n compared with that of the np series. For the np series, because of the relatively large quantum defect of $\delta = 1.38$,[9] the l mixing by the stray or ac field becomes significant only at high Rydberg states of $n > 100$. Therefore, the diabatic ionization behavior of the ionization onset at low n, as a function of the pulsed-field strength, is hardly observed for the MATI peak at the long delay time of ~16 μs.

The one-photon excitation to an nf Rydberg series has rarely been reported for molecules to our best knowledge. This is because the optical selection rule is $\Delta l = \pm 1$ and the angular momentum of the molecular orbital, which is poorly defined, is equal to or less than 1 for many organic molecules although it had been reported that the highest occupied molecular orbital (HOMO) of benzene correlates to a d atomic orbital and nf series is optically active in the MATI spectrum.[18] For $Cr(Bz)_2$, however, the HOMO corresponds to the pure nonbonding d_{z^2} orbital of the central metal atom and thus the angular momentum of $l = 2$ is fairly well defined. The MATI signal represents long-lived high Rydberg states.

These states have high-l quantum numbers, and it results from the l mixing caused by the stray or ac field. However, the initial excitation to the high Rydberg states is governed by the optical selection rule of $\Delta l = \pm 1$. Therefore, the MATI spectrum could be interpreted using the optically bright and dark states with coupling between those as depicted in Fig. 4. Here, optically bright nf and np Rydberg states of $Cr(Bz)_2$ are strongly coupled to optically dark high-l Rydberg states through the l mixing in the presence of the stay and/or ac scrambling field to give the long-lived MATI states. The resultant MATI spectrum then reflects the long-lived high-l Rydberg states as well as optically accessible initial low-l quantum states.

In the overlapping region of $n=80-120$, the MATI signal originated from the nf series decreases as n increases. The lifetime modulation as a function of the principal quantum number had also been observed for NO and Ar.[5,18] Even though the understanding of the origin for the lifetime modulation in Rydberg manifolds of the title molecule may need full consideration of multichannel interactions, a simple interpretation based on the one-electron atomic model could be conceived. That is, as the excitation energy increases, the density of states increases. The increase of the density of states should result in the coupling of the initially prepared f states to higher or lower l states according to the selection rule of $\Delta l = \pm 1$. The extent of the l coupling is strongly dependent on the external electric field, quantum defect, and principal quantum number with a relation of $\delta_l / n^3 = 3n^2 F$.[1] Thus, at the given stray field of F, the mixing of the nf states to high-l states with $\Delta l = +1$ may be activated early at the low n's, whereas the coupling to low-l states with $\Delta l = -1$ becomes significant later at the relatively higher n's. Therefore, in the $n=80-120$ region, the optically dark nd series could be effectively mixed with the optically bright f series, leading to the decrease of the lifetime because of the vulnerable nature of the nd series. At $n > \sim 120$, the np series undergoes the complete l mixing to give rise to the long-lived Rydberg manifolds. This simple picture, however, may need much improvement, especially in terms of the interaction of the Rydberg electron with the ionic core of this large molecule. High-resolution Rydberg spectroscopic work would be quite valuable for unraveling the dynamics involved in the l-mixing process in greater detail for this interesting molecule.

It should be noted that the l mixing by the ac scrambling field is much more effective for the $n=50-100$ Rydberg states. In Fig. 5(a), the MATI signal obtained in the absence of ac scrambling field is shown as a function of the PFI field. The MATI signal due to $n=50-100$ states is significantly diminished, indicating that the corresponding lifetime gets shortened. Meanwhile, the MATI signal due to $n=100-200$ Rydberg states is found out to be less affected by the ac scrambling field. The application of the dc spoil field at the time of laser irradiation cuts off the high n Rydberg states. In Fig. 5(b), the MATI peak shows the redshift as the spoil field increases from 0.01 to 2.55 V/cm. The MATI peak shift due to the spoil field is found to be very significant. The energy shift from the adiabatic IP with increasing the spoil field is found out to be not systematic, and it seems to be nontrivial to extract quantitative values from the experiment carried out under the strong spoil field.

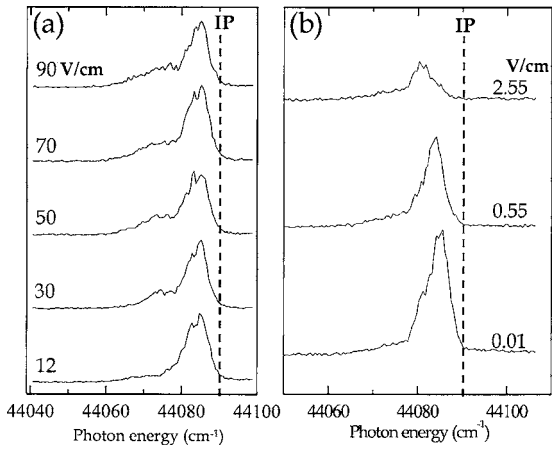

FIG. 5. (a) The MATI spectrum taken as a function of the PFI field in the absence of both ac scrambling and spoil fields. (b) The MATI origin band taken with the application of the various dc spoil fields without the ac scrambling field (see the text).

The $Cr(Bz)_2$ molecule provides the unique opportunity to investigate high n Rydberg states of the complex molecular system. However, at the same time it had been difficult to obtain a well-resolved MATI spectrum partly because of the lack of the knowledge about the ionization behavior of the optically accessible Rydberg states of $Cr(Bz)_2$. In the following section, using the most optimal experimental condition, the MATI spectroscopic characterization of the $Cr(Bz)_2$ cation is given.

B. Vibrational structure of the bis(η^6-benzene) chromium ion

The high-resolution MATI spectrum obtained in this work provides the detailed vibrational structure of the $Cr(Bz)_2$ cation. Since the HOMO is nearly pure d_z^2 orbital of Cr which is not involved in the η bonding between benzene and Cr, the structural change of $Cr(Bz)_2$ induced by the first ionization is not expected to be drastic. The HOMO belongs to a_{1g}, and the Jahn-Teller splitting is not expected for this highly symmetric molecular cation. The neutral and cation structures are calculated using the density functional theory (DFT) (UB3LYP/LANL2DZ) method, Table II. The distance between chromium and benzene is predicted to be increased from 1.680 to 1.701 Å in the ionization process, while the structure of benzene moieties is little changed. The origin band is most strongly observed. The Bz–Cr–Bz symmetric

TABLE II. Structural parameters of bis(η^6-benzene)chromium in the neutral and cationic ground states from the DFT calculation (UB3LYP/LANL2DZ level).

	R(Cr–Bz) (Å)	R(C–C) (Å)	R(C–H) (Å)	∠(CCCH) (deg)
Neutral ground	1.680	1.430	1.085	1.23
Cationic ground	1.701	1.431	1.083	1.30
Difference	0.021	0.001	−0.002	0.07

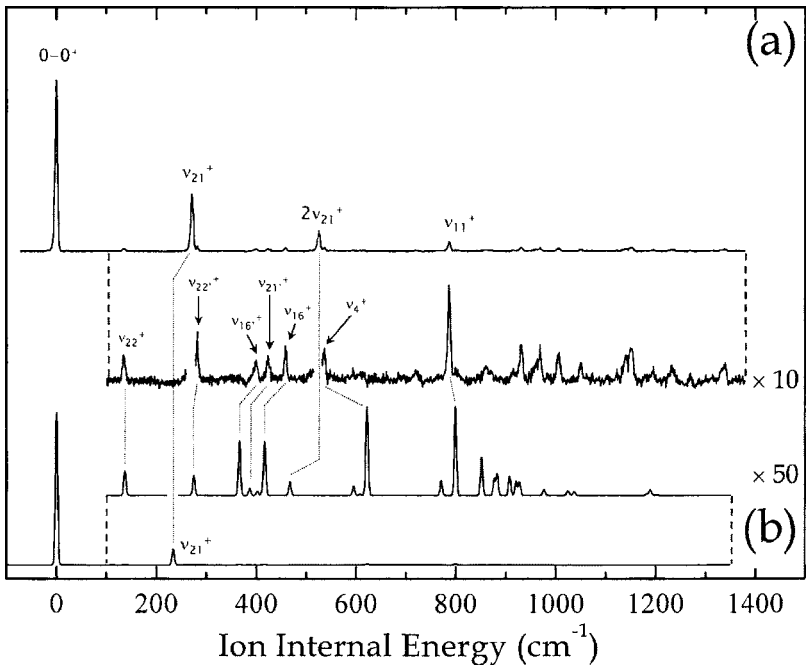

FIG. 6. (a) The MATI spectrum of the bis(η^6-benzene)chromium cation. (b) The simulated spectrum calculated by the Franck-Condon analysis based on DFT calculations for molecular structures and vibrational frequencies.

stretching mode is found to be significantly active in the MATI spectrum, Fig. 6(a). Since the spectrum is very well resolved, vibrational frequencies are quite precisely determined. The Franck-Condon analysis based on *ab initio* molecular structures and vibrational frequencies is carried out to give the simulated MATI spectrum in Fig. 6(b).

Even though relative intensities and peak positions of the simulation do not match with the experiment extremely well, the Franck-Condon simulation leads to the reasonable assignments at least for low-frequency vibrational modes. Firstly, as stated above, the band strongly observed at the vibrational energy of 272 cm^{-1} certainly corresponds to the symmetric Bz–Cr–Bz stretching mode (ν_{21}). This value is ~8 cm^{-1} larger than the earlier reported ZEKE spectroscopic value.[26] The corresponding *ab initio* frequency of 234 cm^{-1} is quite low compared to the experiment. Due to the ionization-driven structural change, the Bz–Cr–Bz stretching mode should be Franck-Condon active, as clearly depicted in Fig. 6(b). The band at 526 cm^{-1} is assigned as the first overtone of the ν_{21} mode. As the fundamental ν_{21} frequency is 272 cm^{-1}, this assignment suggests that the Bz–Cr–Bz stretching mode is quite positively anharmonic. The vibrational band observed at 787 cm^{-1} cannot be ascribed to the second overtone of ν_{21} since the fundamental and first overtone frequencies preclude this possibility which otherwise would give the negative anharmonicity for the ν_{21} mode. The Franck-Condon analysis predicts that the ν_{11} mode associated with C–H out-of-plane bending motion is active in the ionization spectrum, Figs. 6 and 7. The corresponding *ab initio* frequency is 799 cm^{-1}, which is quite close to the experiment. This assignment is in accord with recent reports by Ketkov *et al.*[27,28,34] and Sohnlein and Yang.[26]

Other weakly observed vibrational bands in the MATI spectrum are also well characterized. Because of the high quality of the spectrum, many new vibrational features of the $Cr(Bz)_2$ ion could be identified. The 135 cm^{-1} band (ν_{22}) is assigned to the asymmetric bending motion of benzene moieties of which the calculated value is 137 cm^{-1}. Normal mode descriptions for ν_{21}, ν_{22}, and ν_{11} modes are given in Fig. 7. Other skeletal modes in which the benzene moiety moves like a rigid body along the intermoiety potential energy surfaces are observed in the vibration energy range of 100–500 cm^{-1}. Even though *ab initio* values do not reproduce the experiment perfectly, reasonable assignments based on the Franck-Condon analysis are carried out and listed in Table III. Overall, the experimental vibrational frequencies are higher than those calculated, suggesting that the force constants associated with the Bz–Cr–Bz intermoiety motion are stronger than those predicted by the *ab initio* calculation at the level used in this work. A more reliable calculation at the higher level is desirable for the more thorough understanding of the η-bonding nature of the metal-benzene sandwich complex.

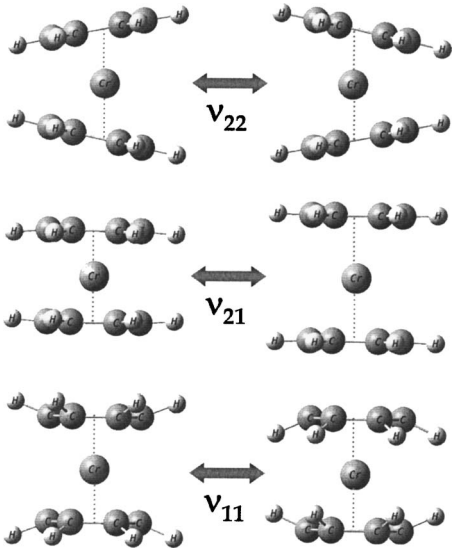

FIG. 7. Normal mode descriptions for ν_{22}, ν_{21}, and ν_{11} modes (see Table III).

TABLE III. Experimental and calculated vibrational frequencies of bis(η^6-benzene)chromium.

Expt.				Calc.[a]			
		Cationic ground					
Neutral ground[b]	Rydberg[c]	ZEKE[d]	MATI[e]	Cationic ground	Assign.[f]	Sym.[g]	Normal mode description
			0		$0\text{-}0^+$		Origin
			135	137	ν_{22}^+	e_{1u}	Sym. Bz–Bz bend.
277	263	264	272	234	ν_{21}^+	a_{1g}	Sym. Cr–Bz str.
			282	275	$\nu_{22'}^+$	e_{1g}	Asym. Bz–Bz bend.
			400	366	$\nu_{16'}^+$	e_{2u}	Bz out-of-plane mode (asym.)
			424	387	$\nu_{21'}^+$	a_{2u}	Asym. Cr–Bz str.
			459	416	ν_{16}^+	e_{2g}	Bz out-of-plane mode (sym.)
	528	527	526	467	$2\nu_{21}^+$	a_{1g}	
			537	622	$\nu_{4''}^+$	$b_{1u}+b_{2g}$	Bz out-of-plane mode (asym.+sym.)
791	790	786	787	799	ν_{11}^+	a_{1g}	Out-of-plane C–H mode (sym.)
			862	852	$\nu_{10'}^+$	e_{1g}	Out-of-plane C–H mode (asym.)
			870	877	ν_{10}^+	e_{1u}	Out-of-plane C–H mode (sym.)
910	920		915	883	ν_{17}^+	e_{2g}	Out-of-plane C–H mode (sym.)
			931	908	$\nu_{17'}^+$	e_{2u}	Out-of-plane C–H mode (asym.)
			968	921	ν_5^+	b_{1u}	Out-of-plane C–H mode (sym.)
			1006	927	$\nu_{5'}^+$	b_{2g}	Out-of-plane C–H mode (asym.)
			1051	977	$\nu_{1''}^+$	$a_{1g}+a_{2u}$	Bz ring breathing (asym.+sym.)
			1140	1025	$\nu_{12'}^+$	b_{2g}	Bz in-plane mode (asym.)
			1152	1037	ν_{12}^+	b_{1u}	Bz in-plane mode (sym.)
			1194	1183	$\nu_{8'}^+$	e_{2u}	In-plane C–H mode (asym.)
			1232	1190	ν_8^+	e_{2g}	In-plane C–H mode (sym.)
	1348		1338	1370	$\nu_{3''}^+$	$a_{2g}+a_{1u}$	In-plane C–H mode (asym.+sym.)

[a]DFT (UB3LYP/LANL2DZ) not-scaled vibrational frequencies.
[b]Raman spectroscopy (Ref. 36).
[c]$3d_z^2$-$R4p_{x,y}$ Rydberg transition (Ref. 34).
[d]ZEKE spectroscopy (Ref. 26).
[e]This work.
[f]$\nu_1-\nu_{20}$ Wilson numbering (Ref. 37) $\nu_{21}-\nu_{22}$ skeletal vibrations (Ref. 34).
[g]Symmetry species in D_{6h}.

The vibrational bands observed above 700 cm^{-1} are associated with the vibrational modes of benzene moieties. Nuclear motions of two benzene moieties are either symmetric or antisymmetric with respect to the inversion symmetry operation and corresponding vibrational modes are rather complicated in terms of associated nuclear motions. Based on the Franck-Condon analysis, the mode assignment is tentatively carried out, Table III. If our assignment is correct, it implies that the experimental frequencies for the vibrational modes of benzene moieties are also higher than predicted by the *ab initio* calculation. High-level *ab initio* calculations on this large metal-benzene sandwich complex system would be quite challenging but should be very valuable.

IV. SUMMARY

Here, we present the high-resolution one-photon MATI spectrum of bis(η^6-benzene)chromium cooled in a jet. The ionization behavior of high n Rydberg states in the presence of the ac scrambling, spoil, and pulsed fields is systematically investigated. Two distinct Rydberg series which behave quite differently with the electric field conditions are experimentally observed. We have assigned those two distinct peaks as p and f series of Rydberg states. This is reasonable considering the fact that the optical excitation is from the nonbonding d orbital of $Cr(Bz)_2$. The ionization potential is accurately measured to be $44\,090\pm3$ cm^{-1}. Vibrational frequencies of the $Cr(Bz)_2$ cation are precisely measured and corresponding modes are assigned properly using the Franck-Condon analysis based on the DFT calculation. Since our spectrum is of high quality, it gives many newly found vibrational features which provide the detailed inter- and intramoiety vibrational structure of this important molecule. *Ab initio* calculation at the level employed in this work was not satisfactory. High-level *ab initio* calculations would be desirable for a more quantitative explanation of the experimental result.

ACKNOWLEDGMENT

This work was financially supported by Korea Research Foundation (KRF-2005-070-C00063).

[1] F. Merkt, Annu. Rev. Phys. Chem. **48**, 675 (1997), and references therein.
[2] F. Merkt, A. Osterwalder, R. Seiler, R. Signorell, H. Palm, H. Schmutz, and R. Gunzinger, J. Phys. B **31**, 1705 (1998).
[3] F. Merkt and H. Schmutz, J. Chem. Phys. **108**, 10033 (1998).
[4] M. Bixon and J. Jortner, J. Chem. Phys. **105**, 1363 (1996).
[5] M. J. J. Vrakking and Y. T. Lee, J. Chem. Phys. **102**, 8818 (1995).
[6] F. Remacle and R. D. Levine, J. Chem. Phys. **104**, 1399 (1996).
[7] L. Y. Baranov, R. Kris, R. D. Levine, and U. Even, J. Chem. Phys. **100**, 186 (1994).
[8] H.-J. Dietrich and K. Müller-Dethlefs, Phys. Rev. Lett. **76**, 3530 (1996).

[9] U. Even, R. D. Levine, and R. Bersohn, J. Phys. Chem. **98**, 3472 (1994).
[10] M. G. H. Boogaarts, I. Holleman, R. T. Jongma, D. H. Parker, G. Meijer, and U. Even, J. Chem. Phys. **104**, 4357 (1996).
[11] M. C. R. Cockett and M. J. Watkins, Phys. Rev. Lett. **92**, 043001 (2004).
[12] G. R. Janik, O. C. Mullins, C. R. Mahon, and T. F. Gallagher, Phys. Rev. A **35**, 2345 (1987).
[13] C. R. Mahon, G. R. Janik, and T. F. Gallagher, Phys. Rev. A **41**, 3746 (1990).
[14] J. Berkowitz and B. Ruscic, J. Chem. Phys. **93**, 1741 (1990).
[15] B. Ruscic and J. Berkowitz, J. Chem. Phys. **93**, 1747 (1990).
[16] K. S. Haber, Y. Jiang, G. Bryant, E. R. Grant, and H. Lefebvre-Brion, Phys. Rev. A **44**, R5331 (1991).
[17] C. Bordas, P. F. Brevet, M. Broyer, J. Chevaleyre, P. Labastie, and J. P. Perrot, Phys. Rev. Lett. **60**, 917 (1988).
[18] J. D. Hofstein, J. G. Goode, and P. M. Johnson, Chem. Phys. Lett. **301**, 121 (1999).
[19] K.-W. Choi, D.-S. Ahn, S. Lee, H. Choi, K.-K. Baeck, S.-U. Heo, S. J. Baek, Y. S. Choi, and S. K. Kim, ChemPhysChem **5**, 737 (2004).
[20] K.-W. Choi, D.-S. Ahn, J.-H. Lee, and S. K. Kim, J. Phys. Chem. A **110**, 2634 (2006).
[21] K.-W. Choi, J.-H. Lee, and S. K. Kim, Chem. Commun. (Cambridge) **2006**, 78.
[22] K.-W. Choi, J.-H. Lee, and S. K. Kim, J. Am. Chem. Soc. **127**, 15674 (2005).
[23] K.-W. Choi, S. K. Kim, D.-S. Ahn, and S. Lee, J. Phys. Chem. A **108**, 11292 (2004).
[24] S. J. Baek, K.-W. Choi, Y. S. Choi, and S. K. Kim, J. Chem. Phys. **118**, 11040 (2003).
[25] S. J. Baek, K.-W. Choi, Y. S. Choi, and S. K. Kim, J. Chem. Phys. **117**, 2131 (2002).
[26] B. R. Sohnlein and D.-S. Yang, J. Chem. Phys. **124**, 134305 (2006).
[27] S. Y. Ketkov, H. L. Selzle, and E. W. Schlag, Organometallics **25**, 1712 (2006).
[28] S. Y. Ketkov, H. L. Selzle, and E. W. Schlag, Isr. J. Chem. **44**, 65 (2004).
[29] E. W. Schlag, *ZEKE Spectroscopy* (Cambridge University Press, Cambridge, 1998), and references therein.
[30] M. J. Frisch, G. W. Trucks, H. B. Shlegel *et al.*, GAUSSIAN 03, Revision B.02, Gaussian, Inc., Pittsburgh, PA, 2003.
[31] F. Duschinsky, Acta Physicochim. URSS **7**, 551 (1937).
[32] A. Peluso, F. Santoro, and G. D. Re, Int. J. Quantum Chem. **63**, 233 (1997).
[33] R. Borrelli and A. Peluso, J. Chem. Phys. **119**, 8437 (2003).
[34] S. Y. Ketkov, H. L. Selzle, and E. W. Schlag, J. Chem. Phys. **121**, 149 (2004).
[35] S. Y. Ketkov, J. C. Green, and C. P. Mehnert, J. Chem. Soc., Faraday Trans. **93**, 2461 (1997).
[36] L. Schäfer, J. F. Southern, and S. J. Cyvin, Spectrochim. Acta, Part A **27**, 1083 (1971).
[37] G. Varsanyi, *Assignments for Vibrational Spectra of Seven Hundred Benzene Derivatives* (Wiley, New York, NY, 1974).